# Detection of Water-Table by Using Ground Penetration Radar (GPR)

Mundher Ali Seger* & Ahmed Fouad Nashait*

Received on: 24/11/2010
Accepted on: 3/2/2011

**Abstract**

Ground penetrating radar, GPR, is a high resolution geophysical method, which is based on the propagation of high frequency electromagnetic waves. The GPR method images structures in the ground that are related to changes in dielectric properties. In sediments, water content primarily causes the changes in dielectric properties. Therefore GPR can be used to estimate underground water-table.

In this study a GPR system has been used successfully to produce a continuous profile of the water table on the (Said Abdullah bin Al-Hassan Shrine) as a study area, which is located in Al-Yousifyah region to the south of Baghdad. Geotechnical field test to underground water determination by the drilling method commonly used to comparing the results between geotechnical field test and GPR test. Thus, GPR has proven to be an effective detection method for underground water level, and can serve as reference for future applications.

**Keywords:** GPR; water-table; soil dielectric permittivity; penetration depth.

## تحديد مستوى المياه الجوفية باستخدام الرادار الفاحص للأعماق

**الخلاصة**

تقنية جهاز فحص الأعماق تعتبر من أهم طرق الفحص الجيوفيزيائي وتتميز بدقة ووضوح عالي، وتعتمد على طريقة أرسال نبضات كهرومغناطيسة عالية التردد. وتعتمد الصور المأخوذة من جهاز فحص الأعماق على تغير خصائص العزل الكهربائي لطبقات سطح الأرض. وبسبب التأثير الكبير للماء على خصائص العزل الكهربائي، لذا يعد جهاز فحص الأعماق من أفضل طرق تخمين عمق المياه الجوفية.

في هذا البحث تم أستخدام تقنية جهاز فحص الأعماق بنجاح تام بعمل مقاطع طولية تبين عمق المياه الجوفية لموقع الدراسة (مرقد السيد عبد الله بن الحسن المثنى بن الأمام الحسن) الواقع في منطقة اليوسفية الى الجنوب من بغداد كمنطقة دراسة تجريبية. بالأضافة الى مسح جهاز فحص الأعماق تم أيجاد عمق المياه الجوفية بالطريقة التقلدية بواسطة الحفر الأختبارية، لغرض عمل مقارنة بين الطريقتين. ومن خلال التحليل والنتائج تبين أن تقنية جهاز فحص الأعماق طريقة فعالة جداً لتحديد عمق المياه الجوفية وبالأمكان أستخدامها لتطبيقات كثيرة أخرى في المستقبل.

## 1. Introduction

Ground penetrating radar is a geophysical measurement technique that has been extensively used to map the relatively shallow subsurface features at scales from kilometers to centimeters.

GPR is a high resolution geophysical method, which is based on the propagation of high frequency electromagnetic waves. The GPR method images structures in the ground that are related to changes in dielectric properties [1].

In sediments, the water content primarily causes the changes in dielectric properties. Water has a great effect on the dielectric permittivity of porous media due to its strong dipole moment. The

* Building and Construction Engineering Department, University of Technology/ Baghdad

presence of even small amount of water will dominate the behavior of the dielectric permittivity of porous media in a multi-fluid system. For example, the dielectric permittivity generally increases along with the moisture content from the ground surface to the saturated zone, since the dielectric permittivity is to a very large degree controlled by the moisture content of the soil medium in the subsurface. Thus, in order to use GPR for hydrogeology applications including moisture content estimation, water table detection, and contaminant detection, it is necessary to understand how water is distributed and how its distribution is related to the soil medium in the subsurface. In general, the water saturation (or moisture content) increases with depth from the ground surface to the water table in the subsurface [2]. Figures (1, 2) and table (1) shows MALA GPR system used in the site location of study area.

## 2. Physical bases of the GPR System

A GPR system consists of an antenna to transmit and receive signals, a control unit to process signals, a graphic recorder to display radar data, and an analog or digital tape recorder to store, process, and play back data.

The GPR method operates by transmitting a very short electromagnetic pulse into the ground using an antenna. The centre frequency is typically in the range of 10-2000 MHz. Abrupt changes in dielectric properties cause parts of the electromagnetic energy to be reflected back to the ground surface, where it is recorded and amplified by the receiving antenna. The recorded signal is registered as amplitude and polarity versus two-way travel time [3].

The electromagnetic wave propagates in air with the speed of light (0.3 m/ns). In the ground the velocity of electromagnetic waves is reduced since it is dependent on the relative dielectric permittivity (εr), the relative magnetic permeability (μr), and the electrical conductivity (σ). The velocity of electromagnetic waves in a host material is given by:

$$v = \frac{c}{\sqrt{\varepsilon_r \, \mu_r \, \frac{1+\sqrt{1+(\sigma / \omega \varepsilon)^2}}{2}}} \quad \ldots(1)$$

Where: (c) is the electromagnetic wave velocity in vacuum (0.3 m/ns), (εr) relative dielectric of material, (ε = εr εo) the dielectric permittivity and (εo) the dielectric permittivity in free space (8.854x1012 f/m), (ω=2πf) the angular frequency, where (f) is frequency, and the expression (σ = ωε) is a loss factor. In non-magnetic (μr =1) low-loss materials, such a clean sand and gravel, (σ = ωε) ≈ 0.

The velocity of electromagnetic waves is reduced to the expression:

$$v = \frac{c}{\sqrt{\varepsilon_r}} \quad \ldots(2)$$

The Equations (1 and 2) show that the velocity of electromagnetic waves propagating in the ground is decreased compared to the velocity in the air. In low-loss (i.e. resistive) materials the maximum decrease is a factor of nine, which is the velocity of electromagnetic waves in fresh water (0.034 m/ns). Several processes lead to a reduction of the electromagnetic signal strength [4].

## 3. Factors Influencing the Penetration Depth of GPR

The penetration depth of GPR is determined by antenna frequency and the electrical conductivity of the earthen materials being profiled [5]. Soils having high electrical conductivity rapidly attenuate radar energy, restrict penetration depths, and severely limit the effectiveness of GPR. The electrical conductivity of soils increases with increasing water, clay and soluble salt contents.

Electrical conductivity is directly related to the amount, distribution, chemical composition, and phase (liquid, solid, or gas) of the soil water [6]. At a given frequency, the attenuation of electromagnetic energy increases with increasing moisture contents [5]. The lack of adequate data on soil moisture and the high spatial and temporal variations in the degree of soil wetness within most soil map units precluded the use of moisture content in the preparation of GPR soil suitability maps. As a consequence, properties selected to prepare these maps principally reflect variations in the clay and soluble salt contents of soils. These properties include clay content and mineralogy, electrical conductivity, sodium absorption ratio, and calcium carbonate and calcium sulfate contents.

Clays have greater surface areas and can hold more water than the silt and sand fractions at moderate and higher water tensions. Because of their high adsorptive capacity for water and exchangeable cations, clays produce high attenuation losses [5]. As a consequence, the penetration depth of GPR is inversely related to clay content. While soils with more than 35 percent clay are restrictive, soils with less than 10 percent clay are generally favorable to deep penetration with GPR.

Soils contain various proportions of different clay minerals (e.g., members of kaolin, mica, chlorite, vermiculite, smectite groups). The size, surface area, cation-exchange capacity (CEC), and water holding capacity of clay minerals vary greatly. Variations in electrical conductivity are attributed to differences in the CEC associated with different clay minerals. Electrical conductivity increases with increasing CEC [7]. Soils with clay fractions dominated by high cation exchange capacity clays (e.g., smectitic and vermiculitic soil mineralogy classes) are more attenuating to GPR than soils with an equivalent percentage of low cation exchange capacity clays (e.g., kaolinitic, gibbsitic, and halloysitic soil mineralogy classes). Soils classified as kaolinitic, gibbsitic, and halloysitic characteristically have low cation-exchange capacity and low base saturation. As a general rule, for soils with comparable clay and moisture contents, greater depths of penetration can be achieved in highly weathered soils of tropical and subtropical regions that have kandic or oxic horizons than in soils of temperate regions that have argillic horizons. Compared with argillic horizons, kandic and oxic horizons have greater concentrations of low activity clays [8].

## 4. Velocity Analysis

Velocity analysis involves determining the velocity of subsurface materials, then converting the reflection travel times to depths. This is most easily done using methods described by Benson. In Benson's approach, he determined the velocity of soils near the subsurface by testing for the relative dielectric constant.

Table (2) represent dielectric constants and propagation of some materials:

Next, Benson interpreted the location of the water table reflection on a processed GPR profile. The depth to the water table was determined from:

$$d_w = \frac{v\, t_w}{2} \qquad \ldots(3)$$

Where:

dw = The depth to the water table.

tr = The two-way travel time to the reflector (taken from the GPR trace).

## 5. Identification of the Water-Table Reflector

The strength of the water-table radar reflector depends on the contrast between the electrical properties of the unsaturated and saturated zones. In coarse-grained sands the capillary fringe is usually abrupt, especially during dry period, because the pore spaces are large and many are essentially noncapillary. The water-table reflector is more pronounced in these deposits, and the position on the graphic record is relatively easy to locate. In the fine-grained materials, the capillary fringe is more gradual because of the presence of smaller, more continuous pore space, and the water-table is less distinct on the graphic record. Also, where reflective startigraphic features are close to the water-table, the water-table reflection is less abrupt, or masked by overlapping reflections [10].

## 6. Data Collection

### (A) Study Site

GPR data has been collected from (Said Abdullah bin Al-Hassan Shrine), site located in Al-Yousifyah region to the south of Baghdad about 25 km as show in Figure (3). Site Coordinates (33° 2' 35.7504" N 44° 15' 39.1381" E). The geological Stratified consist from Clay and silt deposits.

### (B) Conventional underground water survey method

The field investigation consists of drilling (5) boreholes with depth (10) m. A general site plan showing the positions of the required boreholes in figure (4). One of the reasons of Drilling and trial pitting is to establish the general nature of the strata below a site.

The groundwater regime is often not very well determined by ground investigation. Since pore water pressure is usually a very important factor in any engineering calculation, any seepages or inflows into the borehole should be closely monitored. Each time that groundwater is detected, the depth of entry should be measured and the speed of inflow described. Boring should be suspended and groundwater levels observed in an attempt to determine the static groundwater level. Some specifications allow for standing time (i.e. unproductive time) while the groundwater stabilizes in the borehole. Others require that the driller should only suspend work for a maximum of 20 mm. At the end of this period, if the water level is still rising, its depth is to be recorded and drilling recommenced.

Ground water table (G.W.T.) was encountered at different depths depending on the locations of boreholes and its elevation with respect to sea level which was found to be deep as about (2.65 – 2.67) meters from ground surface level.

### (C) Field Work and GPR Data

During September of 2010, GPR measurements were conducted using a physical model that simulated a rising and falling water table in the earth. The GPR data were measured with antenna have center frequency of 500 MHz. Consistent data acquisition instrument setting on the GPR system were used throughout the course of the experiment in order to reduce and facilitate data processing steps. Measurements were made along the 17 profile lines on the grid showing in figure (5). All GPR measurements were made at an equal distance interval along the profile lines (distance based mode) using a survey wheel.

Data acquisition parameters used in the GPR measurements is presented in table (3).

**7. Data Analysis and Results**

**(A) Data processing**

Rad-Explorer software [11] has been used for the data processing in this study, the following steps was applied to the GPR data:

- A correction of the zero time. The zero time may not have been detected precisely by the instrument in the field and should therefore be repacked to ensure correct depths in the profile. Furthermore, drift of the zero time along the profile can occur because of temperature difference between the instrument electronics and the air temperature or damaged cables. The drift causes misalignment of the reflections and the zero time has to be resampling for all traces along the profile.
- If high frequency electromagnetic noise is present in the GPR profile it can be reduced by temporal low pass or band pass filtering.
- A spatial low pass filter also reduces noise as well as enhancing flat or only slightly dipping reflections, plus suppression of rapid changing features like diffraction hyperbolas and steeply dipping reflections. A spatial high pass filter work in the opposite way by enhancing diffraction hyperbolas, steeply dipping reflections and suppressing flat lying reflections. Spatial filters can change the appearance of the data dramatically and must be used with great caution.

**(B) Results of GPR data**

This investigation was done to determine the depth water-table in site location. Although 17 profile lines on the GPR grid were obtained at measurements, only the data from profile line 5 are shown in figures (6-10) because it's passing through borehole.

The GPR system produces a graphic record of the total travel time needed for a signal to pass through the subsurface, reflect off an interface, and return to the antenna. This total or two-way travel time is measured in nanosecond (10-9 sec) and can be converted to a depth if the velocity of signal propagation through the earth material is known.

Velocities of radar signals in unsaturated material were calibrated along the survey lines as observation wells and ponds with known water levels were passed. By use of this method, the average velocity of the signal through the unsaturated zone (v) and the average depth (dw) are calculated according to Equations (2 and 3).

**(C) Analysis of GPR data**

Signal propagation velocities in unsaturated materials were determined in 5 boreholes. The velocities were determined using equation (3), and ranged from 10.352 to 10.695 m/ns, with mean value of 10.553 m/ns. The relative dielectric of unsaturated materials above water-table were determined in these sites using equation (2), and ranged from 7.8683 to 8.3983, with mean value of 8.120. According to analysis results of velocities and relative dielectric and depending on table (2), the unsaturated material above water-table is dry clay.

A plot of depth to water as a function of two-way travel time, figure (11) shows a strong correlation (R2 = 0.973) between two variables that can be described by the equation:

$$D = 2.134 + 0.01\,tw \qquad \textbf{...(4)}$$

A plot of depth to water as a function of velocity, figure (12) shows a strong correlation (R2 = 0.857) between two variables that can be described by the equation:

$$D = 2.039 + 0.01\,v \qquad \textbf{...(5)}$$

## 8. References:


[1] **John M. Reynolds,** "An Introduction to Applied and Environmental Geophysics", Book, John Wiley & Sons Inc. New York, 1997.

[2] **Changryol Kim,** "A Physical Model Experiment on the Hydrological Applications of GPR". Thesis, Ohio State University, 2001.

[3] **Harry M. Jol,** "Ground Penetrating Radar Theory and Applications", Book, Elsevier B.V. Amsterdam, Netherlands, 2009.

[4] **Benson, A. K.,** "Applications of ground penetrating radar in assessing some geological hazards: examples of groundwater contamination, faults, cavities": Journal of Applied Geophysics, 33(1-3), 1995.

[5] **Daniels D. J.,** "Ground Penetrating Radar: 2nd Edition", Book, The Institute of Electrical Engineers, London, United Kingdom, 2004.

[6] **Maser K. R.,** "Condition Assessment of Transportation Infrastructure Using Ground Penetrating Radar", ASCE Journal of Infrastructure Systems, V.2 (2), June, 1996.

[7] **Saarenketo, T.,** "Electrical Properties of Water in Clay and Silty Soils", Journal of Applied Geophysics 40, 1998.

[8] **Soil Survey Staff,** "Soil Survey Manual", US Department of Agriculture - Soil Conservation Service, Handbook No. 18, US Government Printing Office. Washington DC, 1993.

[9] **Marc Loken,** "Current State of the Art and Practice of Using GPR for Minnesota Roadway Applications": Report, Minnesota Local Road Research Board, 2005.

[10] **Shih, S. F., Doolittle J. A., Myrhe, D. L., and Schellentrager, G. W.,** "Using radar for ground water investigation": Journal of Irrigation and Drainage Engineering, V. 112, no. 2, 1986.

[11] **Rad-Explorer, Software and User Manual,** "The software for GPR data processing and interpretation". Mala Geoscience, Moscow, 2005.

**Table (1) Antenna Properties**

| | Antenna, MHz | | | |
|---|---|---|---|---|
| Parameter | 2000 | 800 | 500 | 250 |
| Resolution, m | 0.04-0.08 | 0.2 | 0.5 | 1.0 |
| Depth, m | 1.5-2 | 3-5 | 7-10 | 7-10 |
| Blind zone, m | 0.06 | 0.1-0.2 | 0.25-0.5 | 0.5-1.0 |

**Table (2): dielectric constants and propagation of materials [9]**

| Material | Dielectric Constant (-) | Propagation Velocity (m/s) |
|---|---|---|
| Air | 1 | .30 |
| Ice (Frozen soil) | 4 | .15 |
| Granite | 9 | 0.10 |
| Limestone | 6 | 0.12 |
| Sandstone | 4 | 0.15 |
| Dry sand | 4 to 6 | 0.12 to 0.15 |
| Wet sand | 30 | 0.055 |
| Dry clay | 8 | 0.11 |
| Wet clay | 33 | 0.052 |
| Asphalt | 3 to 6 | 0.12 to 0.17 |
| Concrete | 9 to 12 | 0.087 to 0.10 |
| Water | 81 | 0.033 |
| Metal | $\infty$ | 0 |

**Table (3) Data acquisition parameter for water table experiment**

| **Parameter** | **Value** |
|---|---|
| No. of lines | 17 |
| Amp. | 163.00 |
| Eps. | 90.00 |
| No. of samples per trace | 512 |
| Time window range (ns) | 51.2 |
| Field gain(db) | 7 |

**Figure (1) MALA GPR System used in the site location of study area**

**Figure (2) MALA GPR Instrument part (Antenna, Control Unit, Monitor)**

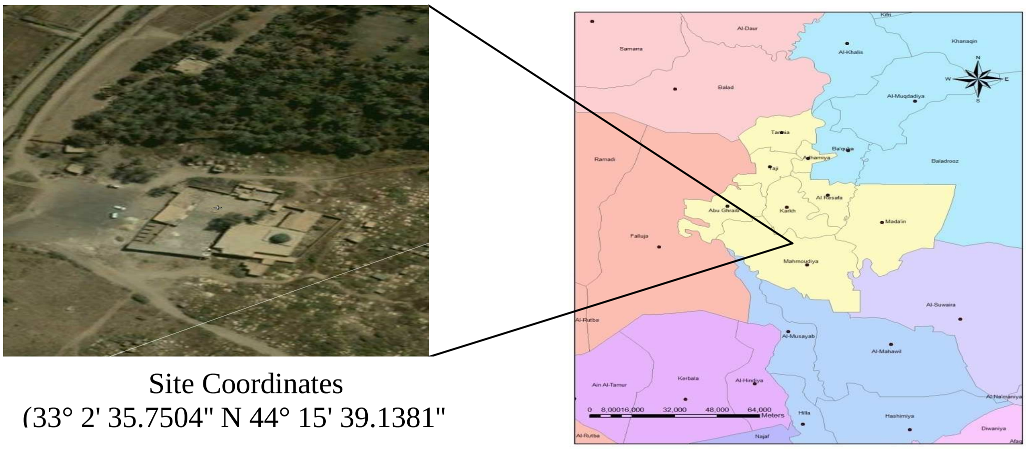


**Figure (3) Aerial photograph for Site**

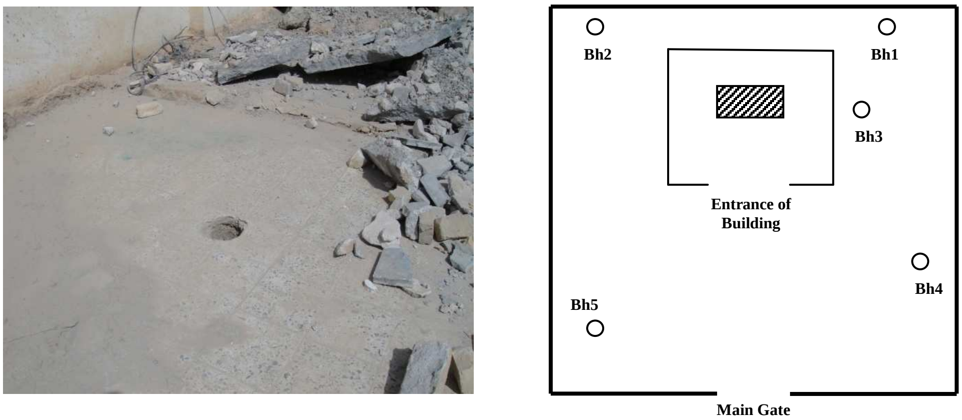


**Figure (4) Position of the required boreholes**

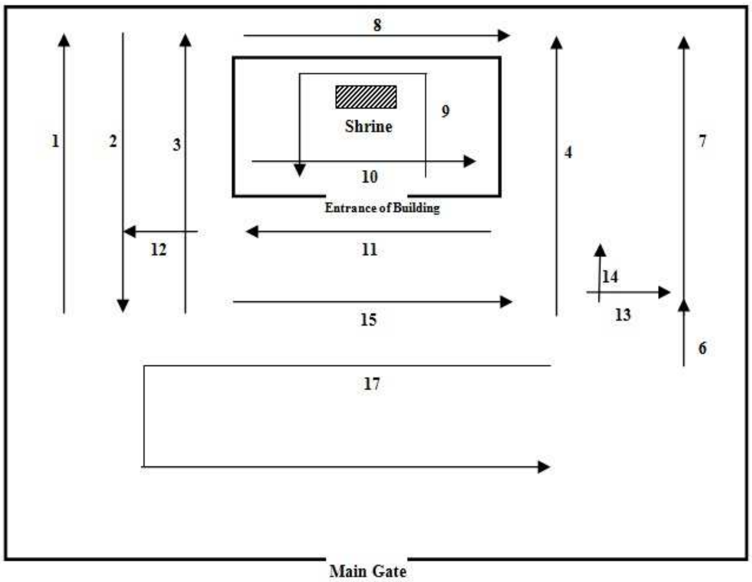


**Figure (5) Site plan and grid line for Said Abdullah shrine site**

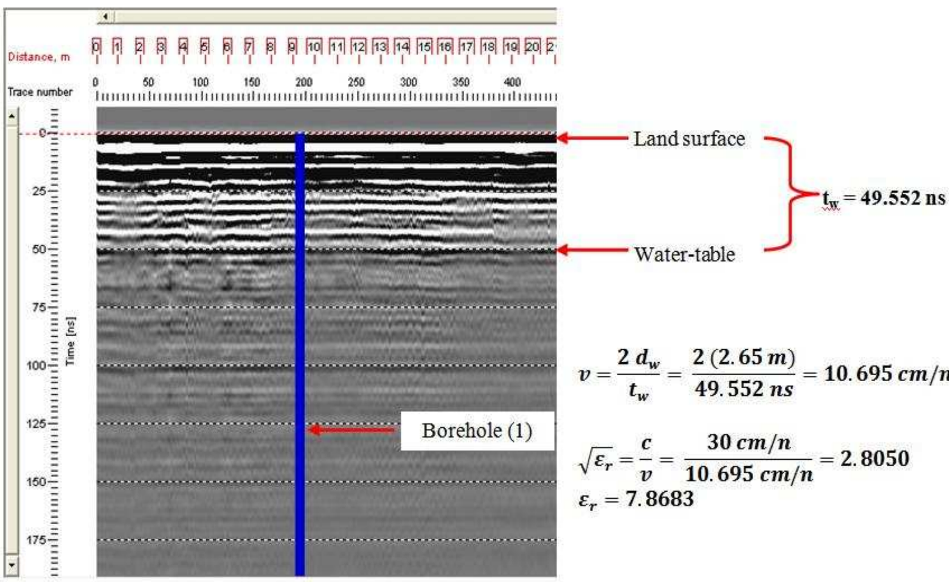


$$v = \frac{2\,d_w}{t_w} = \frac{2\,(2.65\,m)}{49.552\,ns} = 10.695\,cm/ns$$

$$\sqrt{\varepsilon_r} = \frac{c}{v} = \frac{30\,cm/n}{10.695\,cm/n} = 2.8050$$

$$\varepsilon_r = 7.8683$$

**Figure (6) GPR profile images showing (Borehole #1)**

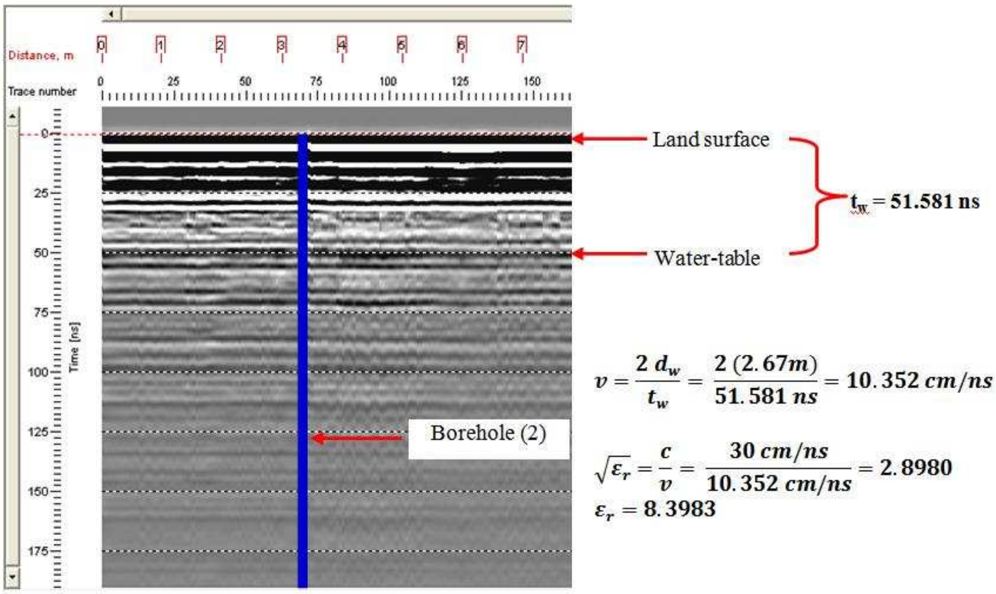


**Figure (7) GPR profile images showing (Borehole #2)**

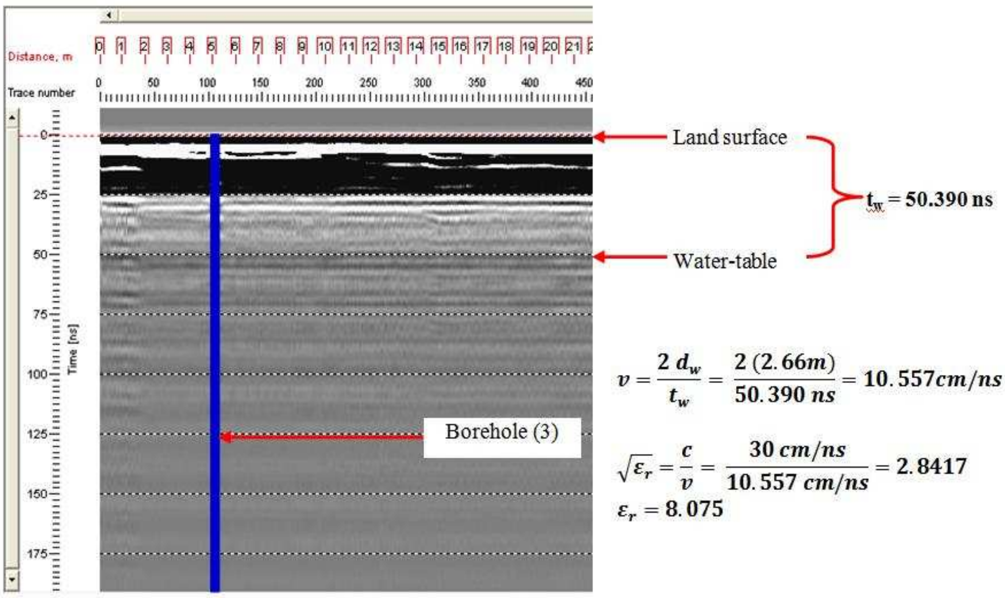


**Figure (8) GPR profile images showing (Borehole #3)**

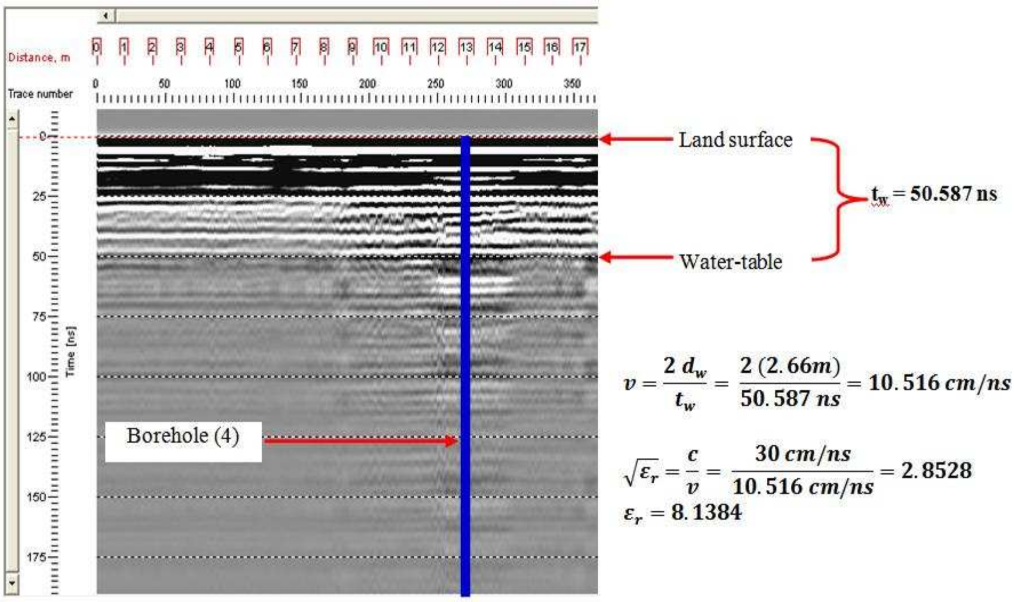


**Figure (9) GPR profile images showing (Borehole #4)**

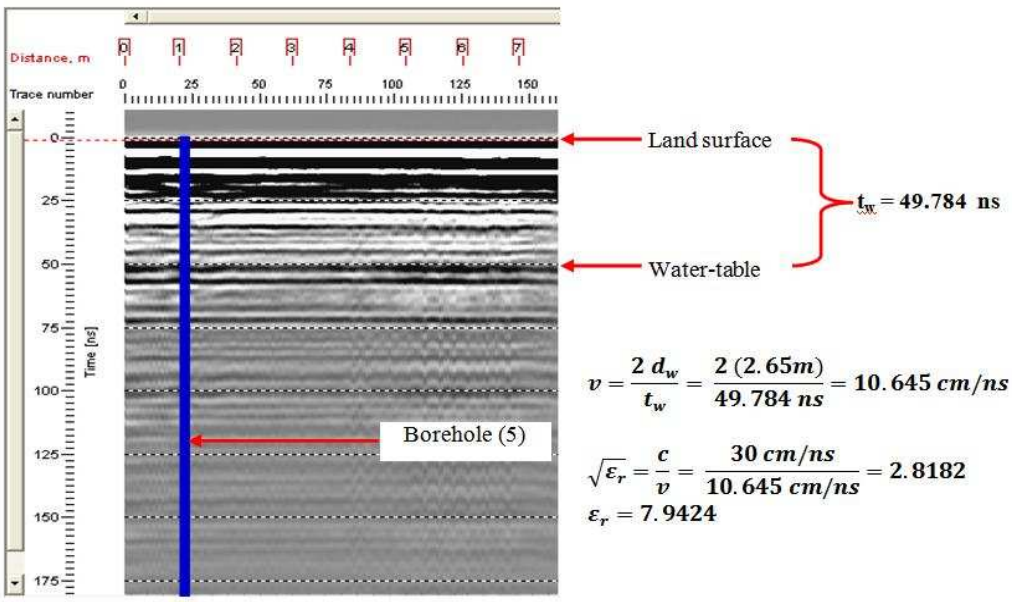


**Figure (10) GPR profile images showing (Borehole #5)**

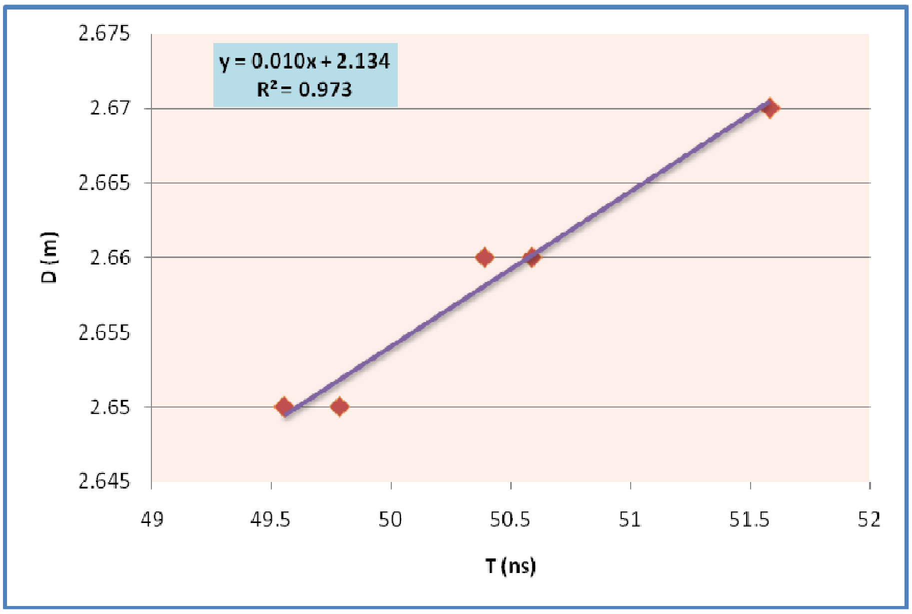


**Figure (11) Relation between two-way travel time and depth of water**

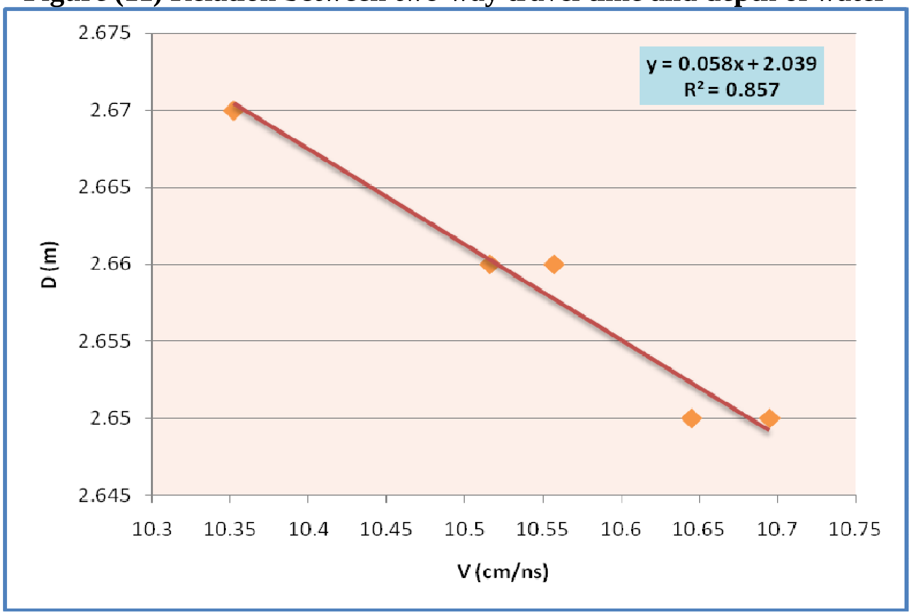


**Figure (12) Relation between velocity and depth of water**